Soft Handoff Analysis of Hierarchical CDMA Cellular Systems

John Y. Kim, *Member, IEEE*, Gordon L. Stüber, *Fellow, IEEE*, Ian F. Akyildiz, *Fellow, IEEE*, and Boo-Young Chung

Abstract—A new soft handoff analysis for hierarchical code-division multiple-access (CDMA) cellular systems is presented. Hierarchical cellular architectures have been proposed to increase cellular system capacity and flexibility. In order to extend such architectures to CDMA-based systems, the performance of soft handoff in hierarchical architectures must be considered. We first develop an analytical method for studying the interference in hierarchical CDMA cellular systems. We then apply the obtained results to a soft handoff analysis model to study the performance of soft handoff in hierarchical architectures. It is observed that dynamic handoff parameter assignment, where parameters are dynamically adjusted according to given interference conditions, offers a more efficient handoff mechanism than fixed handoff parameter assignment.

Index Terms—Active set, carrier-to-interference ratio (CIR), code-division multiple access (CDMA), hierarchical architectures, macrocell, microcell, soft handoff.

NOMENCLATURE

$G_i(r, \theta)$	Link gain between aN MS located at (r, θ) and BS i.
ξ	Gaussian distributed shadowing factor.
$P_{Hij}(r, \theta)$	Probability that aN MS in cell i is connected to BS j given its location (r, θ).
$S_i(j)$	Signal contribution to BS i from MSs located in cell j.
I_i	Total interference power received at BS i.
I_μ	Total interference power received at the microcell.
γ_i	Interference power ratio I_i/I_μ between BS i and the microcell.
$S_{ij}(q, k)$	Interference contribution to BS i from kth MS located in cell q and connected to BS j.
$A(n)$	Active set membership at epoch n.
$P_i(n)$	Probability that BS i is in active set at epoch n.
$B(n)$	BS in active set that minimizes the MS transmit power.
$P_{N \to i}(n)$	Probability that BS i is added to active set at epoch n.
$P_{i \to N}(n)$	Probability that BS i is dropped from active set at epoch n.
$H_{error}(n)$	Handoff error probability at epoch n.

I. INTRODUCTION

SOFT handoff has a special importance in code-division multiple-access (CDMA) cellular systems due to its close relationship to power control. CDMA cellular systems are interference-limited, meaning that their capacities are closely related to the amount of interference they can tolerate. The fundamental idea behind power control is to restrain mobile stations (MSs) and base stations (BSs) from transmitting more power than is necessary in order to limit excess interference. With power control, each MS (or BS) is disciplined to transmit just enough power to meet the target carrier-to-interference ratio (CIR) level. However, in order for power control to work properly, the system must ensure that each MS is connected to the BS having the least path attenuation at all times; otherwise, a positive feedback problem can destabilize the entire system. Soft handoff ensures that each MS is served by the best BS a majority of the time, by allowing connections to multiple BSs with macroscopic selection diversity.

Hierarchical cellular architectures consisting of overlaid macrocells and underlaid microcells have been proposed [3]–[8]. Such architectures are attractive since they can boost system capacity on a per need basis; macrocells can cover large areas with low traffic densities, whereas microcells can cover small areas with high traffic densities. When extending hierarchical system architectures to CDMA based systems, it is important to understand corresponding soft handoff behavior that results from deploying such architectures. As mentioned above, soft handoff has great impact on CDMA cellular system performance/capacity, and studying its performance in hierarchical architectures can provide crucial information on how the system performance can be optimized. Velocity-based handoff schemes, where fast moving MSs are assigned to microcells while slow moving MSs are assigned to microcells, have been proposed [1], [2]. Such schemes can reduce the number of handoffs. However, they may not be suitable for hierarchical CDMA architectures that share the same spectrum in all hierarchical layers, since the interlayer interference can increase sharply. Several studies have been performed on hierarchical CDMA architectures [3]–[8] but none contains an extensive study on soft handoff performance. In [6], the authors suggest a macrodiversity power control scheme which essentially places the entire system traffic in soft handoff mode. Such schemes increase the system performance at the expense of increased handoff signaling overhead and infrastructure cost. The focus of this paper is to devise a new analytical method for studying soft handoff in hierarchical CDMA architectures, whose results can be used to optimize the soft handoff parameters and, hence,

maximize the system capacity while minimizing the handoff signaling overhead.

This paper focuses on the reverse link performance of hierarchical CDMA cellular systems. Our analytical approach is divided into two main parts; interference analysis and handoff analysis. We introduce an interference analysis whose emphasis is on CIR performance and interference imbalance of hierarchical CDMA systems. Introducing microcell(s) to an existing macrocell layer causes an interference imbalance between the layers which can greatly impact the overall system performance. Therefore, it is important to characterize the interference in hierarchical CDMA architectures, and our analysis provides a tool for studying the performance under soft handoff. The second part of this paper introduces a handoff analysis method similar to those proposed in [9] and [10], where a moving MS is tracked to determine its soft handoff active set membership. Such analysis is useful for determining cell boundaries and overall handoff efficiencies for a given set of handoff parameters. The studies in [9] and [10] are limited to single MS and are not accurate when the interference is taken into account. We develop a new soft handoff model to study the performance of soft handoff in the presence of interference. We accomplish this by augmenting a user tracking handoff model with the results obtained from our interference analysis. The resulting model is an excellent and accurate tool for studying the impact of soft handoff parameters on soft handoff performance measures such as handoff error probability and average active set membership. Yet, it is simple to implement and computationally efficient. The paper also studies the effect of dynamic handoff parameter assignment where the handoff parameters are dynamically adjusted based on the given interference conditions. It is observed that dynamic parameter assignment offers a more efficient soft handoff mechanism than fixed assignment by reducing unnecessary soft handoff overhead.

The remainder of this paper is organized as follows. In Section II, we describe our models and corresponding analysis for interference and soft handoff. In Section III, our numerical and analytical results are presented and compared. This paper is concluded with some final remarks in Section IV.

II. SYSTEM MODEL AND ANALYSIS

Our channel model accounts for shadow fading and path loss due to distance.[1] The link gain between an MS located at (r, θ) and BS i is

$$G_i(r, \theta) = d_i(r, \theta)^{-\alpha} 10^{\xi_i/10}$$
$$G_i(r, \theta)_{[\text{dB}]} = -\alpha 10 \log_{10}[d_i(r, \theta)] + \xi_i \quad (1)$$

where $d_i(r, \theta)$ is the distance between the MS and BS i, α is the path loss exponent, and $10^{\xi_i/10}$ is the shadowing component with log-normal distribution

$$\xi_i \sim N(0, \sigma_s^2) \quad (2)$$

[1]One can incorporate Rayleigh/Nakagami fading into our analysis by using a log-normal approximation for the composite log-normal Rayleigh/Nakagami distribution [11].

where σ_s is the shadow standard deviation. Therefore, $G_i(r, \theta)$ also has log-normal distribution

$$G_i(r, \theta)_{[\text{dB}]} \sim N(-\alpha 10 \log_{10}[d_i(r, \theta)], \sigma_s^2) \ . \quad (3)$$

Since our analysis involves a multicell system, our propagation model also accommodates shadow correlation between the multiple BS links

$$\mathrm{E}[\xi_i \xi_j] = \rho \sigma_s^2, \quad i \neq j \ . \quad (4)$$

A. Interference Analysis

Our system model consists of three macrocells and single microcell embedded within the macrocell layer as shown in Fig. 1. Our analysis can easily be extended to system models with larger cell deployments. The macrocells and microcell both use omnidirectional BS antennas. The microcell location is specified by the distance d_μ and angle θ_μ with respect to BS 1. Each macrocell area contains N MSs, and the microcell area contains M MSs. The MSs are assumed to be uniformly distributed within each cell area. It is important to realize that the MSs located within a macro- or microcell area are not necessarily served by the BS located at the center of that macro- or microcell. Moreover, our model is not restricted to uniform macrocells either. Different MS densities within the macrocells can be realized by assigning different values of N to the macrocells and, likewise, by assigning different values of M to the microcells should there be more than one microcell. The purpose of this paper is to develop a model for evaluating the effects of interference imbalance on soft handoff performance. The introduction of the microcell in Fig. 1 will introduce interference imbalance into the overall system. Additional interference imbalance can be introduced by assigning different values of N to the macrocells as well. However, for exemplary purposes, we will assume that each macrocell area contains N uniformly distributed MSs.

Suppose that each MS connects to the BS that provides the least attenuation link. Given the location of an MS r and θ in Cell 1, the probability that the MS is connected to BS i is

$$\begin{aligned}
\mathrm{P}_{\text{H1}i}(r, \theta) &= \mathrm{P}[G_i(r, \theta) \geq G_j(r, \theta), \ j = 1, 2, 3, \mu] \\
&= \int_{-\infty}^{\infty} \frac{1}{\sqrt{2\pi}\sigma_s} \exp\left[-\frac{(\xi_i - \mu_i(r, \theta))^2}{2\sigma_s^2}\right] d\xi_i \\
&\quad \prod_{j \neq i} \Phi\left(\frac{\xi_i - \mu_j(r, \theta) - \rho[\xi_i - \mu_i(r, \theta]}{\sqrt{(1 - \rho^2)}\sigma_s}\right)
\end{aligned}$$
$$(5)$$

where $\Phi(x) = 1 - (1/2)\text{erfc}(x/\sqrt{2})$. Therefore, the probability of an MS in Cell 1 being connected to BS i is

$$\mathrm{P}_{\text{H1}i} = \int_0^{2\pi} \frac{d\theta}{2\pi} \int_0^{R_\text{M}} \frac{2r \, dr}{R_\text{M}^2} \mathrm{P}_{\text{H1}i}(r, \theta) \quad (6)$$

where R_M is the macrocell radius. Similarly, we can calculate P_{H2}, P_{H3}, and $\mathrm{P}_{\text{Hmicro}}$ for the MSs located in different cells.
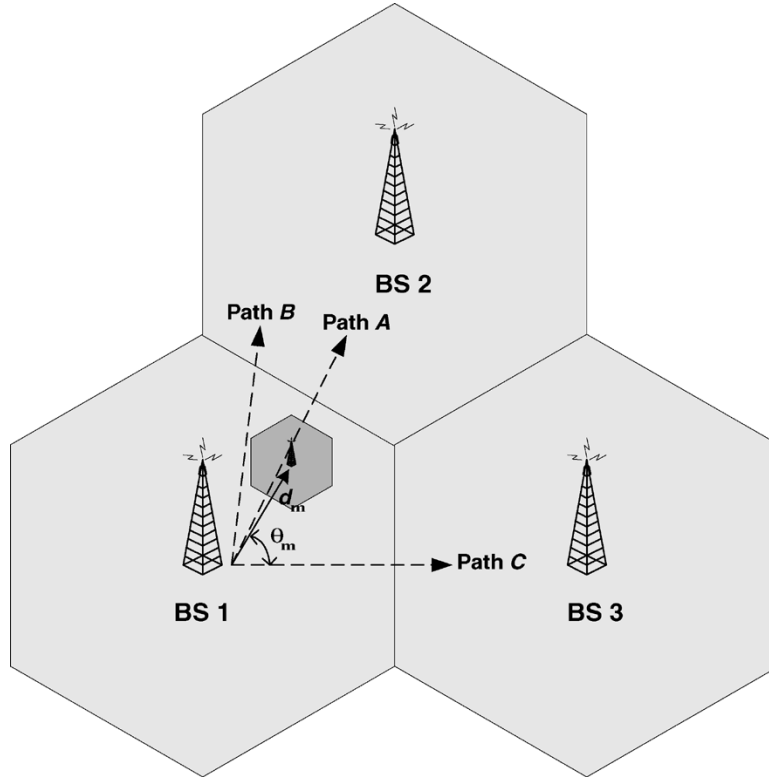
Fig. 1.   Hierarchical system model.

It may be argued that (5) is not representative of CDMA systems that employ power control and soft handoff. For these systems, an MS will connect to the BS that minimizes the transmit power required to achieve a target CIR. Looking at this another way, if an MS were to transmit with fixed power P_T, it would connect to the BS that provides the largest CIR. Hence, under the assumption of ideal soft handoff, (5) becomes

$$
\begin{aligned}
\mathrm{P}_{\mathrm{H}1i}(r,\theta) &= \mathrm{P}[\mathrm{CIR}_i(r,\theta) \geq \mathrm{CIR}_j(r,\theta), \ \ j=1,2,3,\mu] \\
&= \mathrm{P}\left[\frac{G_i(r,\theta)P_T}{I_i} \geq \frac{G_j(r,\theta)P_T}{I_j}, \ \ j=1,2,3,\mu \right] \\
&= \mathrm{P}\left[\frac{G_i(r,\theta)}{\gamma_i} \geq \frac{G_j(r,\theta)}{\gamma_j}, \ \ j=1,2,3,\mu \right].
\end{aligned}
\tag{7}
$$

We will show in Section III-C that, in terms of our handoff analysis, there is barely any difference between the two approaches. Moreover, our results will show that handoff errors sometimes occur where MSs fail to connect to their ideal BSs. So an analysis based on ideal soft handoff is really an approximation as well. For these reasons, we will continue with our interference analysis based on (5). In the sequel, our approach will be justified by extending our analysis to ideal soft handoff, using (7) in place of (5).

The total reverse link signal power received by BS i is equal to the sum of contributions from MSs located in different cells

$$
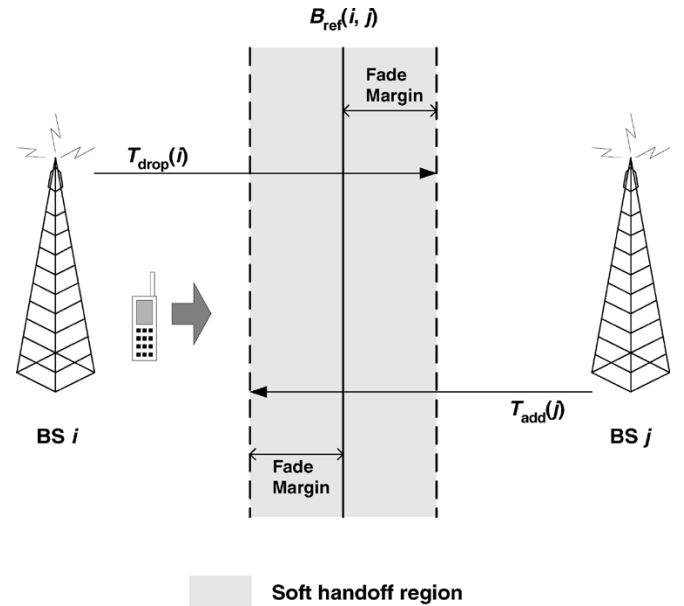S_i = S_i(1) + S_i(2) + S_i(3) + S_i(\mu)
\tag{8}
$$

Fig. 2.   Soft handoff parameters and corresponding handoff region.

where $S_i(j)$ is the signal contribution to BS i from MSs located in cell j. With the introduction of a microcell, the level of interference that each BS experiences I_i will be uneven. Let γ_i be the interference power ratio between BS i and the microcell

$$
\gamma_i = \frac{I_i}{I_\mu}.
\tag{9}
$$

Assuming a uniform CIR requirement and perfect power control, the signal power that is received from a MS connected to BS i must satisfy

$$C_i = \gamma_i C_\mu \tag{10}$$

where C_μ is the power-controlled received power level of a MS connected to the microcell, which is used as a reference. Therefore

$$I_i = S_i - C_i. \tag{11}$$

We now investigate the signal contributions from MSs in the same cell, but connected to different BSs. Let N_{ij} ($M_{\mu j}$) be the number of MSs in cell i (microcell) connected to BS j

$$N = N_{i1} + N_{i2} + N_{i3} + N_{i\mu}$$
$$M = M_{\mu 1} + M_{\mu 2} + M_{\mu 3} + M_{\mu\mu}. \tag{12}$$

We define $\mathbf{N_i}$ as a vector containing N_{ij}

$$\mathbf{N_i} = [N_{i1} \ N_{i2} \ N_{i3} \ N_{i\mu}]. \tag{13}$$

Let us consider $S_1(1)$ as an example. Given $\mathbf{N_1}$

$$S_1(1) = N_{11}C_1 + \sum_{k=1}^{N_{12}} S_{12}(1, k)$$
$$+ \sum_{l=1}^{N_{13}} S_{13}(1, l) + \sum_{p=1}^{N_{1\mu}} S_{1\mu}(1, p) \tag{14}$$

where $S_{ij}(q, k)$ is the interference contribution to BS i from the kth MS located in cell q and connected to BS j. Under the assumption of perfect power control

$$S_{ij}(q, k) = \frac{G_i(r, \theta)}{G_j(r, \theta)} C_j \ , \ \ 0 < S_{ij}(q, k) < C_j. \tag{15}$$

The cumulative distribution function of $S_{ij}(q, k)$ for all k, $S_{ij}(q)$, is then

$$F_{S_{ij}(q)}(z)$$
$$= \frac{1}{P_{Hqj}} \int_0^{2\pi} \frac{d\theta}{2\pi} \int_0^{R_M} \frac{2r\,dr}{R_M^2}$$
$$\times P\left[\frac{G_i(r, \theta)}{G_j(r, \theta)} C_j < z | \text{MS is connected to BS } j\right]$$
$$= \frac{1}{P_{Hqj}} \int_0^{2\pi} \frac{d\theta}{2\pi} \int_0^{R_M} \frac{2r\,dr}{R_M^2}$$
$$\times \int_{-\infty}^{\infty} \times \frac{1}{\sqrt{2\pi}\sigma_s} \exp\left[-\frac{(\xi_j - \mu_j(r, \theta))^2}{2\sigma_s^2}\right] d\xi_j$$
$$\times \Phi\left(\frac{\xi_j - 10\log_{10}\left[\frac{C_j}{z}\right] - \mu_i(r, \theta) - \rho[\xi_j - \mu_j(r, \theta)]}{\sqrt{(1-\rho^2)}\sigma_s}\right)$$
$$\times \prod_{l \neq i,j} \Phi\left(\frac{\xi_j - \mu_l(r, \theta) - \rho[\xi_j - \mu_j(r, \theta)]}{\sqrt{(1-\rho^2)}\sigma_s}\right). \tag{16}$$

Since $S_{ij}(q)$ is a nonnegative random variable, its expected value and the second moment are given as follows:

$$E[S_{ij}(q)] = \int_0^\infty [1 - F_{S_{ij}(q)}(z)]dz$$
$$= \int_0^{C_j} [1 - F_{S_{ij}(q)}(z)]dz$$
$$E[S_{ij}^2(q)] = \int_0^{C_j} 2z[1 - F_{S_{ij}(q)}(z)]dz \tag{17}$$

where $\text{Var}[S_{ij}(q)] = E[S_{ij}^2(q)] - E[S_{ij}(q)]^2$. Then, given $\mathbf{N_1}$, the mean and variance of $S_1(1)$ are

$$E[S_1(1)|\mathbf{N_1}] = N_{11}C_1 + N_{12}E[S_{12}(1)] + N_{13}E[S_{13}(1)]$$
$$+ N_{1\mu}E[S_{1\mu}(1)]$$
$$E[S_1^2(1)|\mathbf{N_1}] = N_{12}\text{Var}[S_{12}(1)] + N_{13}\text{Var}[S_{13}(1)]$$
$$+ N_{1\mu}\text{Var}[S_{1\mu}(1)] + N_{11}^2 C_1^2 + N_{12}^2 E[S_{12}(1)]^2$$
$$+ N_{13}^2 E[S_{13}(1)]^2 + N_{1\mu}^2 E[S_{1\mu}(1)]^2$$
$$+ \sum_{i=1} N_{1i}E[S_{1i}]\left(\sum_{j \neq i} N_{1j}E[S_{1j}]\right). \tag{18}$$

The N_{1j} are binomial random variables with parameters P_{H1j}. Applying the chain rule of probability

$$E[S_1(1)] = \sum_{N_{11}=0}^N \binom{N}{N_{11}} P_{H11}^{N_{11}}(1 - P_{H11})^{N-N_{11}}$$
$$\times \sum_{N_{12}=0}^{N-N_{11}} \binom{N - N_{11}}{N_{12}} \bar{P}_{H12}^{N_{12}}(1 - \bar{P}_{H12})^{N-N_{11}-N_{12}}$$
$$\times \sum_{N_{13}=0}^{N-N_{11}-N_{12}} \binom{N - N_{11} - N_{12}}{N_{13}}$$
$$\times \bar{P}_{H13}^{N_{13}}(1 - \bar{P}_{H13})^{N-N_{11}-N_{12}-N_{13}} E[S_1(1) \mid \mathbf{N_1}]$$
$$= \sum_{N_{11}=0}^N \sum_{N_{12}=0}^{N-N_{11}} \sum_{N_{13}=0}^{N-N_{11}-N_{12}} \frac{N!}{N_{11}!N_{12}!N_{13}!N_{1\mu}!}$$
$$\times P_{H11}^{N_{11}}(1 - P_{H11})^{N-N_{11}} \bar{P}_{H12}^{N_{12}}(1 - \bar{P}_{H12})^{N-N_{11}-N_{12}}$$
$$\times \bar{P}_{H13}^{N_{13}}(1 - \bar{P}_{H13})^{N_{1\mu}} E[S_1(1) \mid \mathbf{N_1}]$$
$$E[S_1^2(1)] = \sum_{N_{11}=0}^N \sum_{N_{12}=0}^{N-N_{11}} \sum_{N_{13}=0}^{N-N_{11}-N_{12}} \frac{N!}{N_{11}!N_{12}!N_{13}!N_{1\mu}!}$$
$$\times P_{H11}^{N_{11}}(1 - P_{H11})^{N-N_{11}} \bar{P}_{H12}^{N_{12}}(1 - \bar{P}_{H12})^{N-N_{11}-N_{12}}$$
$$\times \bar{P}_{H13}^{N_{13}}(1 - \bar{P}_{H13})^{N_{1\mu}} E[S_1^2(1) \mid \mathbf{N_1}] \tag{19}$$

where

$$\text{Var}[S_1(1)] = E[S_1^2(1)] - E[S_1(1)]^2$$
$$\bar{P}_{H12} = \frac{P_{H12}}{P_{H12} + P_{H13} + P_{H1\mu}}$$
$$\bar{P}_{H13} = \frac{P_{H13}}{P_{H13} + P_{H1\mu}} \ . \tag{20}$$

Similarly, we can calculate the means and variances of $S_1(2)$, $S_1(3)$, and $S_1(\mu)$. Therefore

$$
\begin{aligned}
E[S_1] &= E[S_1(1)] + E[S_1(2)] + E[S_1(3)] + E[S_1(\mu)] \\
\text{Var}[S_1] &= \text{Var}[S_1(1)] + \text{Var}[S_1(2)] + \text{Var}[S_1(3)] + \text{Var}[S_1(\mu)] \\
E[I_1] &= E[S_1] - C_1 \\
\text{Var}[I_1] &= \text{Var}[S_1] \ .
\end{aligned}
\tag{21}
$$

We can model I_1 as either a Gaussian or log-normal random variable [12]. Subsequently, we can compute the characteristics of I_2, I_3, and I_μ. We run our analysis in the following iterative steps.

```
1) Set C_1 = C_2 = C_3 = C_μ.
2) Compute means and variances of I_1, I_2,
   I_3, and I_μ.
3) Compute E[γ_i] = E[I_i/I_μ].
4) Set C_i = E[γ_i]C_μ.
5) Goto Step 2).
```

We have experimentally verified that less than 15 iteration loops are needed to converge on the γ. Then the reverse link CIR becomes

$$
\text{CIR} = \frac{C_i}{I_i} = \frac{C_\mu}{I_\mu}.
\tag{22}
$$

B. Soft Handoff Analysis

In CDMA-based systems, each BS transmits a pilot signal to assist soft handoff [13]. MSs use the pilot signals to initiate and complete handoffs among other things. An *active set* refers to a set of BSs to which an MS is connected at any given time. The active set contains multiple BSs when the MS is in soft handoff mode.

Suppose that the active set membership is based on the received pilot signal power.[2] The upper threshold T_{add} is the pilot signal level where qualifying BSs are added to the active set, whereas the lower threshold T_{drop} determines when the BSs are removed from the active set. The difference between T_{add} and T_{drop} is an indicator of how long a soft handoff will take on average. This is graphically illustrated in Fig. 2. Considering an MS that is traveling from BS i to BS j, the soft handoff region is determined by T_{drop} imposed on BS i and T_{add} imposed on BS j. We determine the values of T_{add} and T_{drop} by defining the reference boundary B_{ref} and adding a fade margin to combat the effect of shadow fading [14].

In this section, we introduce a hierarchical soft handoff analysis similar to the analysis presented in [9] and [10], which tracks a moving MS to observe its active set membership while incorporating the spatial correlation property of shadow fading. However, the previous studies are limited to single traveling

[2]CDMA cellular systems actually use the forward link E_c/I_o, the ratio of the received pilot chip energy to total interference spectral density, to determine active set memberships. For the present, we will use received pilot signal power instead, and in Section III-C illustrate the difference between these two methods for determining active set membership in terms of their soft handoff performance.

MS and may not be accurate when the interference is taken into account. As previously mentioned, the introduction of microcell(s) into a macrocell layer results in interference imbalance which can impact the soft handoff decisions and performance. A handoff analysis based on received pilot signal strength and single MS only does not accurately depict the actual system behavior. However, we realize that a comparable analysis that includes multiple MSs while incorporating interference effects is prohibitively complicated and computationally exhaustive. Therefore, we introduce a new soft handoff analysis model which allows us to study soft handoff performance in conjunction with interference performance, by integrating the results obtained in our interference performance study. Our analysis accurately depicts the handoff performance of hierarchical systems, yet has the advantage of being computationally efficient. We omit some detailed derivations of our analysis in the following section, referring the reader to [9] and [10].

According to Gudmundson [15], log-normal shadowing can be modeled as a Gaussian white noise process that is filtered with a first-order low-pass filter

$$
\xi_i(n) = \varepsilon \xi_i(n-1) + (1-\varepsilon)\xi
\tag{23}
$$

where

$$
\begin{aligned}
\xi &\sim N(0, \bar{\sigma}^2) \\
\sigma_{\text{s}}^2 &= \frac{1-\varepsilon}{1+\varepsilon}\bar{\sigma}^2.
\end{aligned}
\tag{24}
$$

Then the correlation function of shadowing becomes

$$
\begin{aligned}
E[\xi_i(n+k)\xi_i(n)] &= \sigma_{\text{s}}^2 \varepsilon^k \\
&= \sigma_{\text{s}}^2 \varepsilon_D^{[d_i(n+k)-d_i(n)]/d_o}
\end{aligned}
\tag{25}
$$

where ε_D and d_o are the correlation parameters.

We now consider an MS traveling a certain path and study its active set membership. Let $A(n)$ be the active set membership at epoch n for the MS under consideration. Let $P_i(n)$ be the probability that BS i is in active set at epoch n

$$
P_i(n) = P[\text{BS } i \in A(n)].
\tag{26}
$$

When $A(n)$ contains more than two BSs, the MS connects to the BS in the set which minimizes its transmit power, thereby limiting interference. This means that the BS selection within the set depends not only on the forward link received pilot strengths but also the reverse link interference conditions. Let $B(n)$ be the BS in the active set that minimizes the MS transmit power. Since $A(n)$ is constantly being updated, the selection of $B(n)$ is based on the active set membership at epoch $n-1$

$$
\begin{aligned}
B(n) &= \max\left\{ \frac{G_i(n)}{I_i(n)} \,\middle|\, \text{BS } i \in A(n-1) \right\} \\
&= \max\left\{ \frac{G_i(n)}{\gamma_i(n)} \,\middle|\, \text{BS } i \in A(n-1) \right\}.
\end{aligned}
\tag{27}
$$

As mentioned before, CDMA systems measure the forward link E_c/I_o to determine the active set memberships. However, for now we just use the received pilot signal strength. We also assume that the BSs transmit their pilot signals with equal power.

TABLE I
COMPARISON OF ANALYTICAL AND NUMERICAL RESULTS. MICROCELL LOAD (M) IS FIXED AT 12 WHILE MACROCELL LOAD (N) IS VARIED

N	M	Simulation				Analysis			
		E[CIR]	E[γ_1]	E[γ_2]	E[γ_3]	E[CIR]	E[γ_1]	E[γ_2]	E[γ_3]
12	12	-12.70 dB	0.135	0.096	0.093	-12.70 dB	0.136	0.096	0.090
13	12	-12.86 dB	0.148	0.110	0.107	-12.86 dB	0.148	0.108	0.102
14	12	-13.03 dB	0.162	0.128	0.125	-13.01 dB	0.160	0.120	0.115
15	12	-13.19 dB	0.176	0.145	0.142	-13.16 dB	0.171	0.134	0.129
16	12	-13.34 dB	0.188	0.163	0.162	-13.30 dB	0.183	0.149	0.143
17	12	-13.50 dB	0.203	0.181	0.182	-13.44 dB	0.195	0.164	0.159
18	12	-13.64 dB	0.219	0.204	0.208	-13.58 dB	0.207	0.180	0.177
19	12	-13.79 dB	0.232	0.225	0.229	-13.72 dB	0.219	0.198	0.195

TABLE II
COMPARISON OF ANALYTICAL AND NUMERICAL RESULTS. MACROCELL LOAD (N) IS FIXED AT 12 WHILE MICROCELL LOAD (M) IS VARIED

N	M	Simulation				Analysis			
		E[CIR]	E[γ_1]	E[γ_2]	E[γ_3]	E[CIR]	E[γ_1]	E[γ_2]	E[γ_3]
12	10	-12.25 dB	0.164	0.141	0.138	-12.23 dB	0.164	0.126	0.120
12	11	-12.48 dB	0.146	0.113	0.111	-12.47 dB	0.146	0.109	0.103
12	12	-12.70 dB	0.135	0.096	0.093	-12.70 dB	0.136	0.096	0.090
12	13	-12.92 dB	0.122	0.084	0.080	-12.92 dB	0.126	0.085	0.079
12	14	-13.13 dB	0.117	0.074	0.070	-13.13 dB	0.117	0.077	0.071
12	15	-13.34 dB	0.105	0.067	0.063	-13.33 dB	0.109	0.070	0.065
12	16	-13.53 dB	0.100	0.062	0.058	-13.52 dB	0.102	0.064	0.059
12	17	-13.72 dB	0.093	0.057	0.053	-13.71 dB	0.096	0.059	0.054

A BS is added to an MS's active set when its path gain exceeds its add threshold $T_{\text{add}}(i)$. Therefore, the probability that it will be added to active set at epoch n is

$$P_{N \to i}(n) = P[G_i(n) > T_{\text{add}}(i) \mid \text{BS } i \notin A(n-1)]. \quad (28)$$

A BS is dropped from active set by using both absolute and relative thresholds. First, the associated path gain must fall below the absolute drop threshold $T_{\text{drop}}(i)$. When it does, its gain is compared to the largest path gain in the active set $B(n)$. When the difference between the two exceeds the relative drop threshold $T_{\text{rel}}(i)$, the BS is dropped from the active set. The relative threshold causes a BS to be dropped from the active set only when its link has deteriorated far below the best link. This also ensures that active set contains at least one candidate BS at all times. The probability that BS i is dropped from active set at epoch n is

$$P_{i \to N}(n) = P[B(n) - G_i(n) > T_{\text{rel}}(i),$$
$$G_i(n) < T_{\text{drop}}(i) \mid \text{BS } i \in A(n-1)]. \quad (29)$$

Finally

$$P_i(n) = P_i(n-1)[1 - P_{i \to N}(n)]$$
$$+ [1 - P_i(n-1)]P_{N \to i}(n). \quad (30)$$

The main purpose of soft handoff is to ensure that the MS is connected to the BS which minimizes its transmit power. Therefore, a handoff error occurs when $B(n)$ is not the best available choice

$$H_{\text{error}}(n)$$
$$= P\left[B(n) \neq \max\left\{\frac{G_1(n)}{I_1(n)}, \frac{G_2(n)}{I_2(n)}, \frac{G_3(n)}{I_3(n)}, \frac{G_\mu(n)}{I_\mu(n)}\right\}\right]$$
$$= P\left[B(n) \neq \max\left\{\frac{G_1(n)}{\gamma_1(n)}, \frac{G_2(n)}{\gamma_2(n)}, \frac{G_3(n)}{\gamma_3(n)}, G_\mu(n)\right\}\right]. \quad (31)$$

Another measure of soft handoff efficiency is the average number of BSs in active set at epoch n, $\bar{A}(n)$

$$\bar{A}(n) = P_1(n) + P_2(n) + P_3(n) + P_\mu(n). \quad (32)$$

A smaller value of $\bar{A}(n)$ implies a lower infrastructure overhead to support soft handoff.

III. NUMERICAL RESULTS

A path loss exponent $\alpha = 4$ and shadow standard deviation $\sigma_s = 8$ dB are used in the simulation. The radii of the macrocell and microcell regions are set to 1500 and 100 m, respectively. Other important simulation parameters include:

- $\varepsilon_D = 0.82$;
- $d_o = 100$ m;
- MS velocity = 60 km/h;
- sampling period = 1 s;
- $T_{\text{rel}} = 3$ dB.

A. Interference Results

Tables I and II show the average CIR and interference performance comparisons between our analytical and simulation results. The microcell is placed at $d_\mu = 600$ m and $\theta_\mu = \pi/3$. Table I contains the results for varying macrocell load N, while Table II shows the results when the microcell load M is varied. It is observed that our analytical and simulation results are in very close agreement, for both E[CIR] and E[γ_i]. It is also seen that the accuracy of our analytical results improves as the interference discrepancy between the layers increases (smaller γ_i). As expected, increasing the system load (N and M) results in a decrease in system CIR performance since it causes the overall interference to increase. Since the density of MSs in the microcell is higher than the density of MSs in the macrocell by nature, the microcell experiences a higher level of interference than the
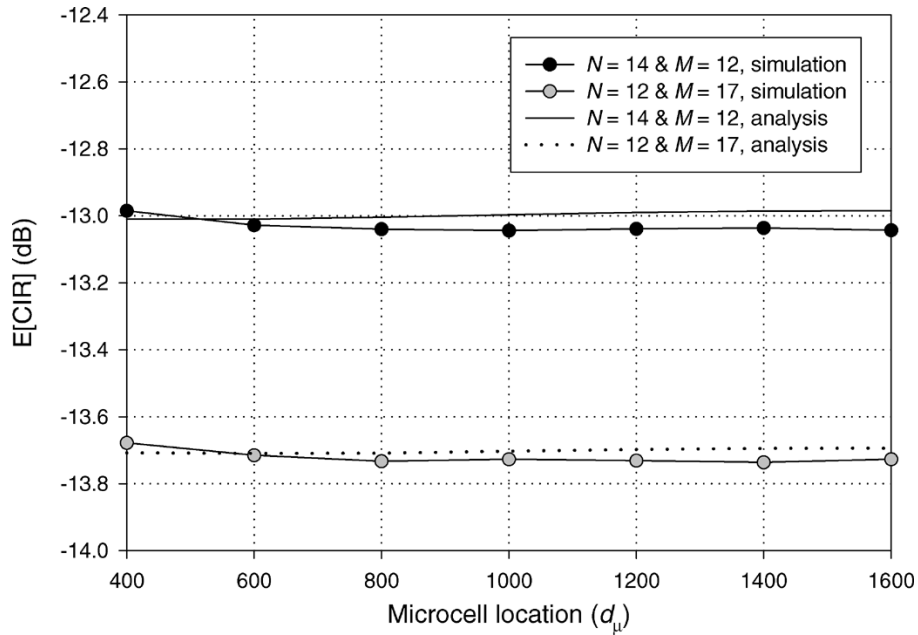
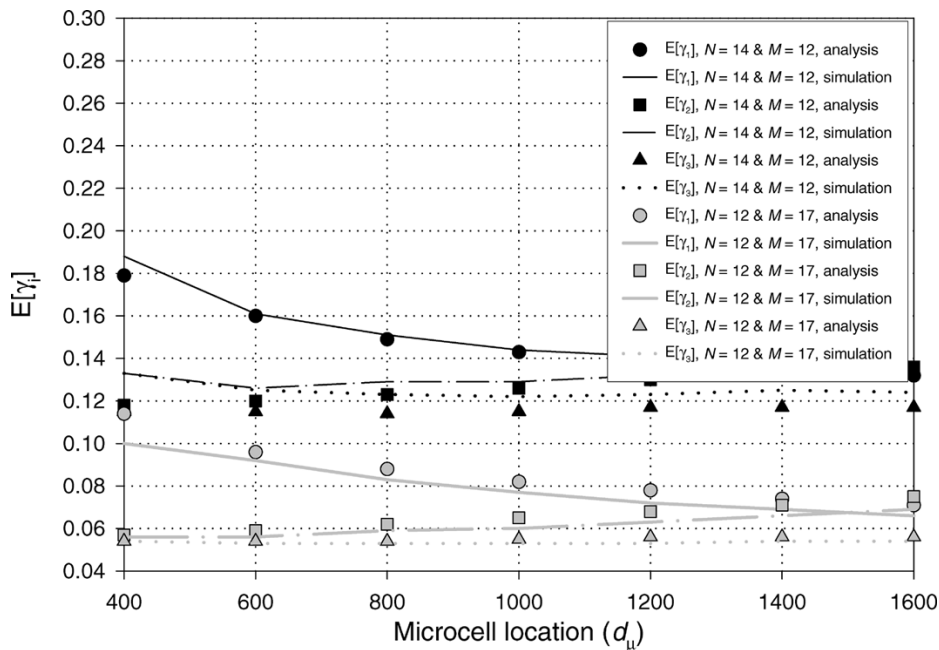Fig. 3.   Average CIR performance vs. microcell location.

Fig. 4. $E[\gamma_i]$ versus microcell location.

macrocells. The γ_i indicate the degree of interference imbalance between the hierarchical layers, and the obtained results agree with our basic intuition; a larger microcell load increases the interference imbalance (smaller γ_i) while a smaller macrocell load decreases the interference imbalance (larger γ_i).

Figs. 3 and 4 show the effect of microcell location on the average CIR and interference performances. The results are obtained by varying d_μ while θ_μ is fixed at $\pi/3$. Again, we observe that our analytical results are in close agreement with the simulation results. Fig. 3 shows that the average CIR performance varies insignificantly with changes in microcell location, although it seems to benefit somewhat from diversity gain when the microcell is located very close to a macrocell BS. Fig. 4 shows how the γ_i are affected by different microcell locations.

It is observed that the corresponding γ_i increase as the microcell moves closer to a macrocell BS. This is expected since the level of interlayer interference between the microcell and macrocell increases as the microcell gets closer to a macrocell BS, which in turn causes the macrocell interference to increase. Observe from Fig. 4 that as d_μ increases γ_1 decreases while γ_2 and γ_3 increase.

B. Soft Handoff Results

We have shown in the previous section how various system loads and microcell locations affect the interference condition of hierarchical CDMA systems. The resulting interference imbalance factors (γ_i) are important parameters in determining the soft handoff performance since, along with the received pilot
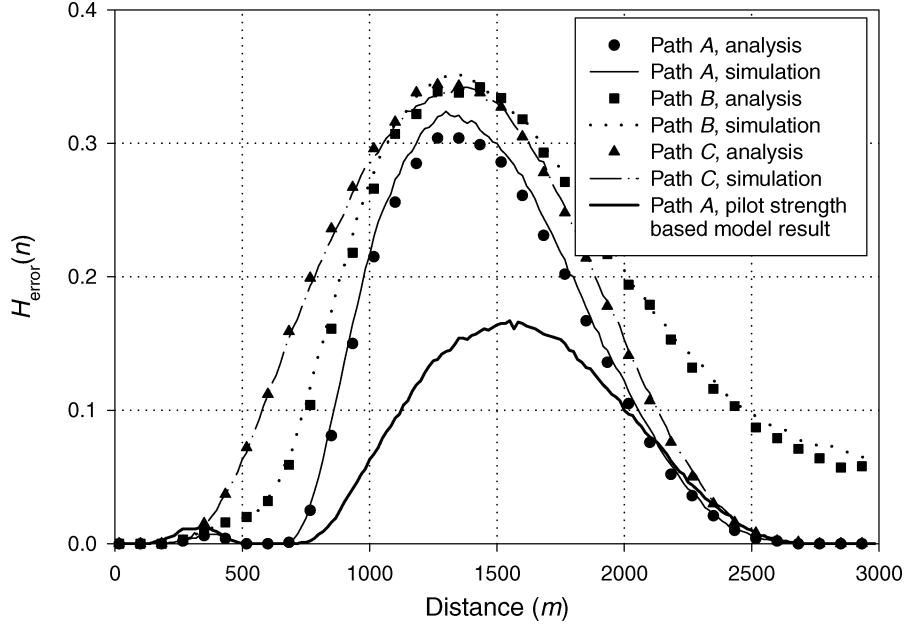
Fig. 5. Error performance of fixed handoff parameter assignment; $N = 13$ and $M = 12$.

signal strengths, they can be used to portray the system behavior during soft handoff and provide information on how to improve the handoff performance. We first examine a fixed parameter handoff algorithm where the values of T_{add} and T_{drop} are fixed regardless of changing interference conditions. In fixed parameter assignment, T_{add} and T_{drop} are determined by defining B_{ref} at an equal distance location and assigning a fade margin of 8 dB[3]

$$T_{\mathrm{add}}(i) = B_{\mathrm{ref}}(i,j) + 8 \text{ dBW}$$
$$T_{\mathrm{drop}}(j) = B_{\mathrm{ref}}(i,j) - 8 \text{ dBW}. \qquad (33)$$

Fig. 5 shows the handoff error probability for fixed handoff parameter assignment. The microcell is located at $d_\mu = 600$ m and $\theta_\mu = \pi/3$. The analytical results are obtained using $\mathrm{E}[\gamma_i]_{\mathrm{analytical}}$ while the simulation results are obtained using actual γ_i. The figure shows the handoff error probability for three traveling paths, all starting from BS 1 as shown in Fig. 1. It is observed that our analytical and simulation results are in good agreement. Fig. 5 also shows the handoff error probability for pilot strength based handoff algorithm [9], [10] and shows how it grossly underestimates the actual handoff error probability when interference levels are not uniform. By incorporating our interference results, our model gives a far more accurate performance analysis than the pilot strength based handoff model. The handoff error probability is observed to increase around the vicinity of physical cell boundaries. It is also observed that the handoff error probability is significantly higher between 1000 and 2000 m. This phenomenon is largely due to our selection of σ_s and T_{drop} for BS 1 ($T_{\mathrm{drop}}(1)$). We have set $T_{\mathrm{drop}}(1)$ so that BS 1 is dropped from the active set once the MS enters the microcell. However, with σ_s set to 8 dB and with the effect of γ_1, BS 1 provides the best connection at the 1000–2000 m region significant number of times, and that

is why one sees high values of $H_{\mathrm{error}}(n)$. The handoff error probability can be improved by relaxing $T_{\mathrm{drop}}(1)$ to cover the region, but that will definitely increase $\bar{A}(n)$, thereby leading to additional system resource requirements. However, the handoff error depends on the microcell location as shown in Fig. 6. The figure contains the error probability plots for path A at three different microcell locations. It is seen that the handoff error probability decreases if d_μ is increased without changing $T_{\mathrm{drop}}(1)$.

Now we examine the performance of dynamic handoff parameter assignment. In dynamic parameter assignment B_{ref} is not fixed, but is dynamically updated as a function of the γ_i to improve the handoff performance. The concept is similar to that of "cell breathing" [16], [17], where a heavily loaded cell shrinks its size to force handoffs and reduce interference. In our case the objective is to control the microcell handoff region according to given interference imbalance condition (as defined by the γ_i) to limit unnecessary overhead. This is accomplished by defining $B_{\mathrm{ref}}(i,\mu)$ at the equilibrium point d_e, where

$$\frac{d_e^{-\alpha}(\mu)}{\gamma_i} = d_e^{-\alpha}(i) \qquad (34)$$

where $d_e(i)$ is the distance between d_e and BS i. It is easily observed that $B_{\mathrm{ref}}(i,\mu)$ moves toward the microcell BS as γ_i decreases, which reduces the microcell soft handoff region accordingly. Fig. 7 compares the performance between fixed and dynamic parameter assignment for path A with the microcell location at $d_\mu = 600$ m and $\theta_\mu = \pi/3$. While dynamic handoff parameter assignment does not offer any significant gain in handoff error probability, it provides a more efficient handoff mechanism over fixed handoff parameter assignment by reducing $\bar{A}(n)$. Fixed handoff parameter assignment requires a larger system overhead since it does not incorporate the system interference information into its handoff decisions. Dynamic handoff parameter assignment dynamically adjusts

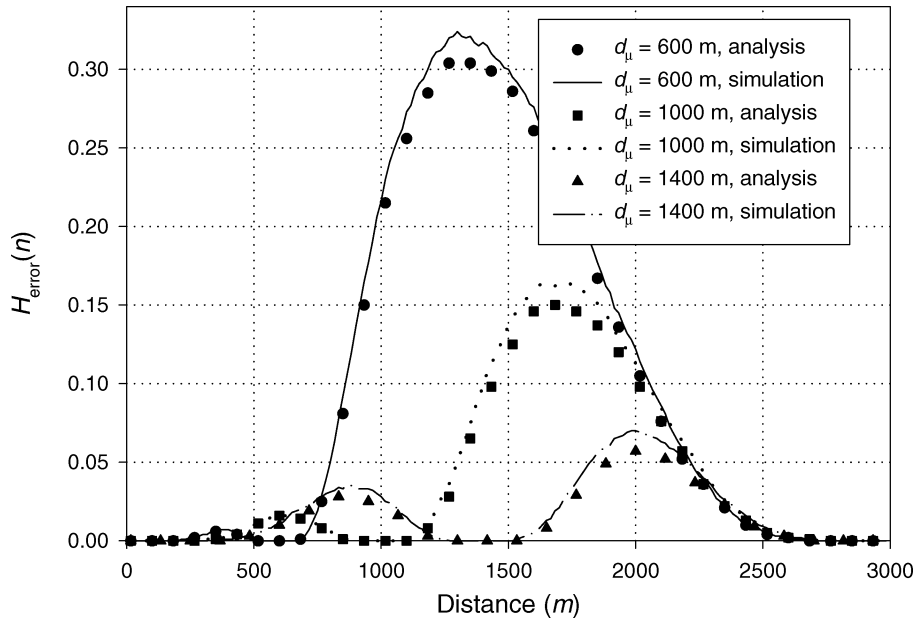---

[3]Other fade margins can be chosen.

Fig. 6.   Effect of microcell location on soft handoff performance; $N = 13$ and $M = 12$.
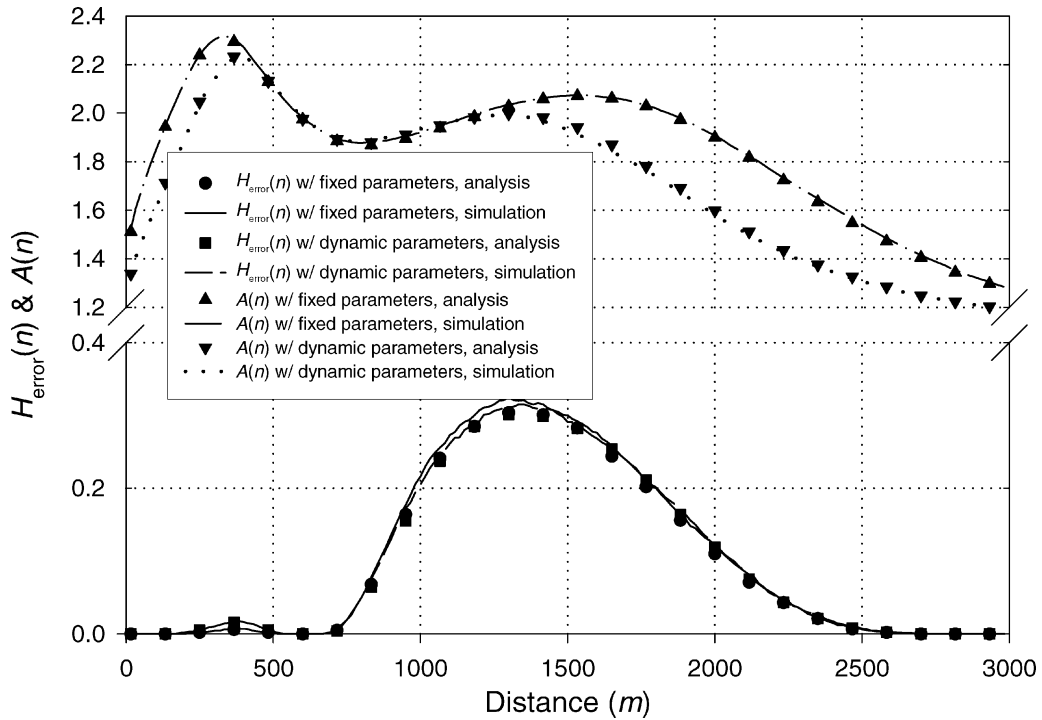

Fig. 7.   Performance comparison between fixed and dynamic handoff parameter assignments; $N = 13$ and $M = 12$.

TABLE III
COMPARISON OF FIXED AND DYNAMIC SOFT HANDOFF PARAMETER
ASSIGNMENT PERFORMANCES; $N = 13$ AND $M = 12$

Path	Fixed		Dynamic	
	$\mathrm{E}[H_{\mathrm{error}}(n)]$	$\mathrm{E}[\bar{A}(n)]$	$\mathrm{E}[H_{\mathrm{error}}(n)]$	$\mathrm{E}[\bar{A}(n)]$
A	0.1043	1.8618	0.1033	1.7135
B	0.1598	1.7573	0.1584	1.6013
C	0.1406	1.8366	0.1314	1.6510

the microcell handoff region so that the system can prevent MSs from being prematurely subjected to soft handoff. Table III

shows the average error probability and active set membership for three specified MS paths. For all three paths, dynamic handoff parameter assignment provides superior performance in $\mathrm{E}[\bar{A}(n)]$ while slightly improving $\mathrm{E}[H_{\mathrm{error}}(n)]$.

Figs. 8 and 9 compare the performance of fixed and dynamic handoff parameter assignment as the system load is varied. As we have observed in Figs. 3 and 4, increasing the macrocell load N increases the γ_i, while increasing the microcell load M reduces the γ_i. It is seen that $\mathrm{E}[\bar{A}(n)]$ stays nearly uniform with various system loads for fixed handoff parameter assignment while it changes according to changes
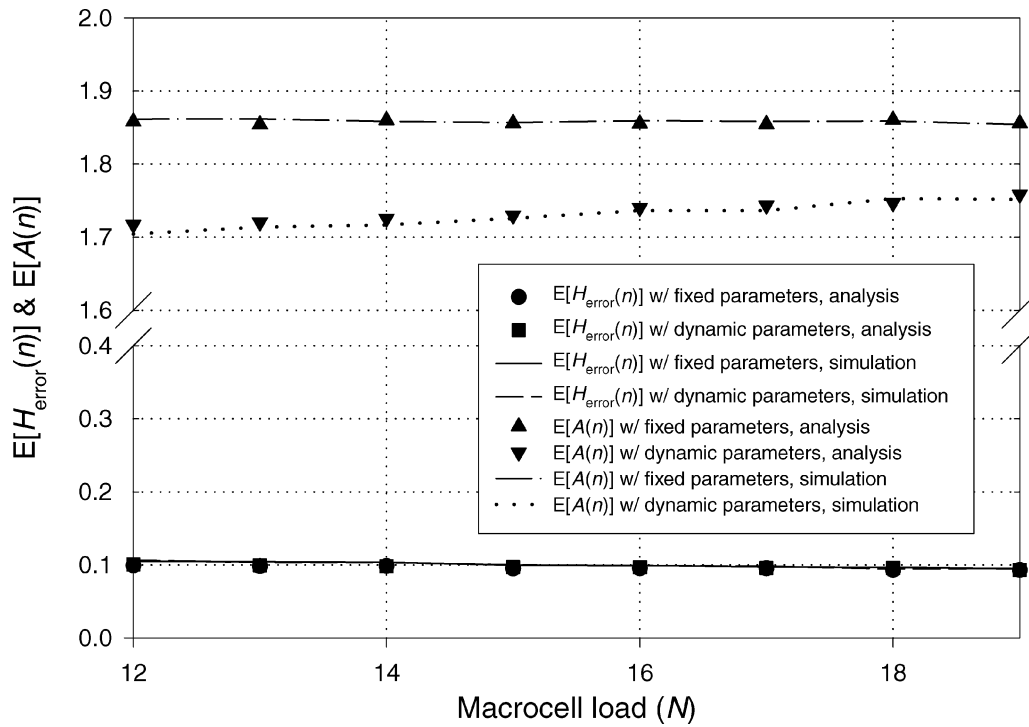
Fig. 8. Effect of interference imbalance on soft handoff performance. Microcell load (M) is fixed at 12 while macrocell load (N) is varied.
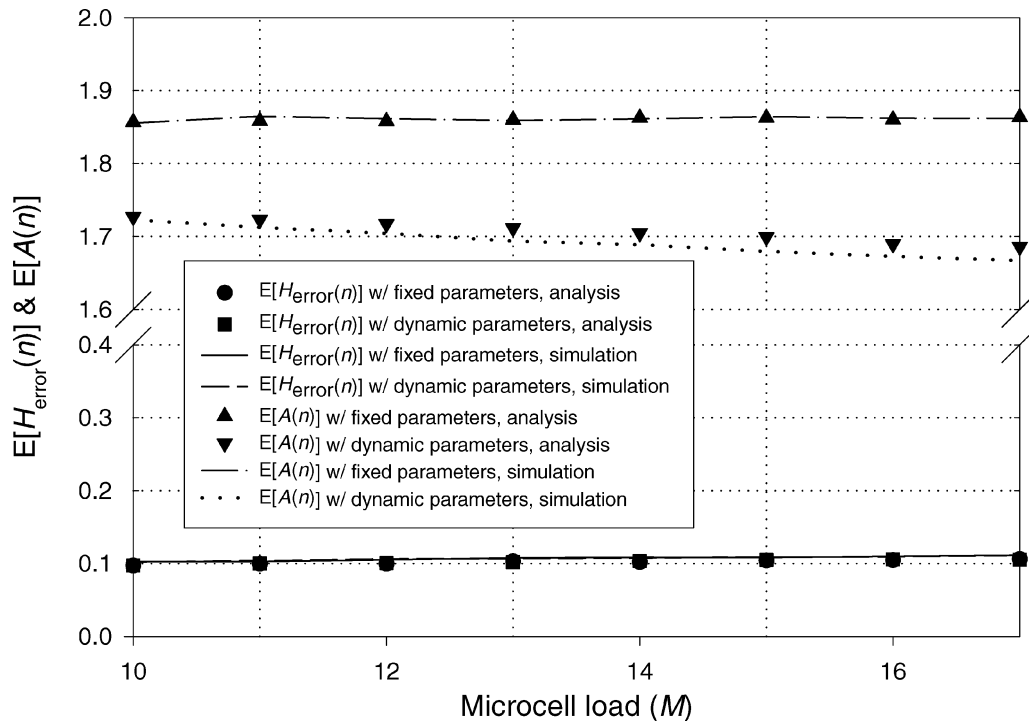

Fig. 9. Effect of interference imbalance on soft handoff performance. Macrocell load (N) is fixed at 12 while microcell load (M) is varied.

in the γ_i for dynamic handoff parameter assignment. As expected, a larger interference imbalance (lower γ_i) causes the microcell handoff region to shrink and thereby reducing $E[\bar{A}(n)]$ for dynamic handoff parameter assignment. The average handoff error probabilities for both fixed and dynamic handoff parameter assignments do not change significantly with varying system load.

C. Ideal Handoff and E_c/I_o Based Active Set Membership

We have made some simplifying assumptions regarding soft handoff and its active set membership in our analysis. In this section, we examine the validity of our assumptions by comparing our results with the results obtained without some of these assumptions.
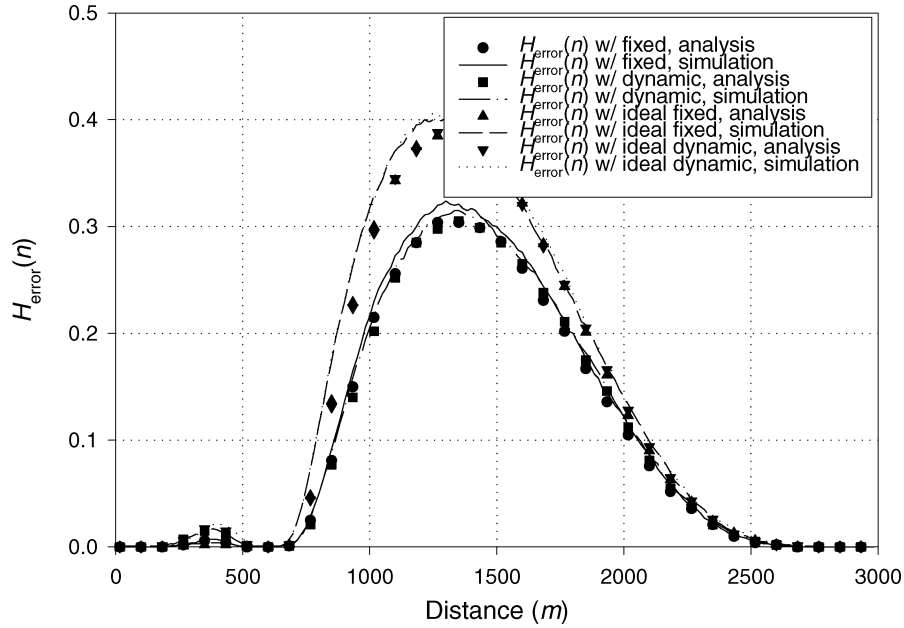
Fig. 10.   Error performance comparison between our soft handoff assumption and ideal soft handoff; $N = 13$ and $M = 12$.
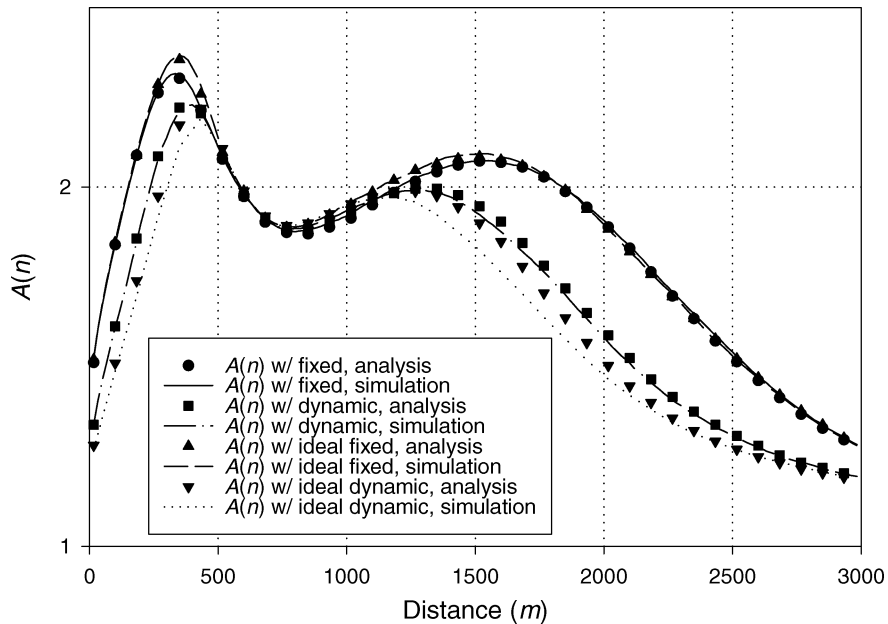

Fig. 11.   Handoff overhead comparison between our soft handoff assumption and ideal soft handoff; $N = 13$ and $M = 12$.

In Section II-A, we assumed that an MS connects to the BS that provides the most robust path gain according to (5). However, during ideal soft handoff, an MS connects to the BS which minimizes its transmit power according to (7). Figs. 10 and 11 compare the handoff error and the active set membership performance between our handoff analysis based on (5) and ideal soft handoff based on (7). There is no significant performance difference between the two approaches. Also, dynamic handoff parameter assignment yields a more efficient handoff mechanism than fixed handoff parameter assignment in either case.

In Section II-B, we used the forward link received pilot signal power to determine active set memberships, while practical CDMA systems use forward link E_c/I_o measurements instead. We now examine the difference between these two approaches.

Let $P_T(i)$ be the total forward transmit power from BS i, including its pilot power. Then, for an MS located at (r, θ)

$$\frac{E_c(i)}{I_o(i)} \approx \frac{G_i(r,\theta)P_{\text{pilot}}}{\sum\limits_{j=1}^{2,3,\mu} G_j(r,\theta)P_T(j)} G_{\text{spread}}. \qquad (35)$$

There are two main difficulties when incorporating E_c/I_o into our analysis. First, it is difficult to model the E_c/I_o behavior mathematically. A power controlled forward link is harder to model than its reverse link counterpart, especially with open loop power control. Second, the total forward transmit power from each BS $P_T(i)$ depends on the number of MSs served by that BS including the MSs in soft handoff. Once again, our system model in Fig. 1 introduces interference imbalance on the
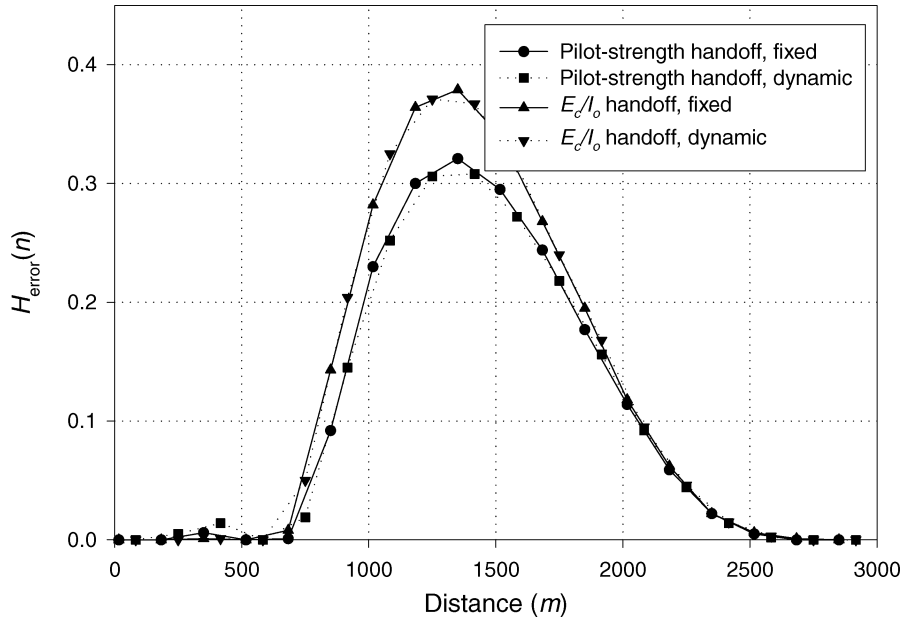
Fig. 12.   Error performance comparison between pilot-strength and E_c/I_o based active set membership; $N = 13$ and $M = 12$.
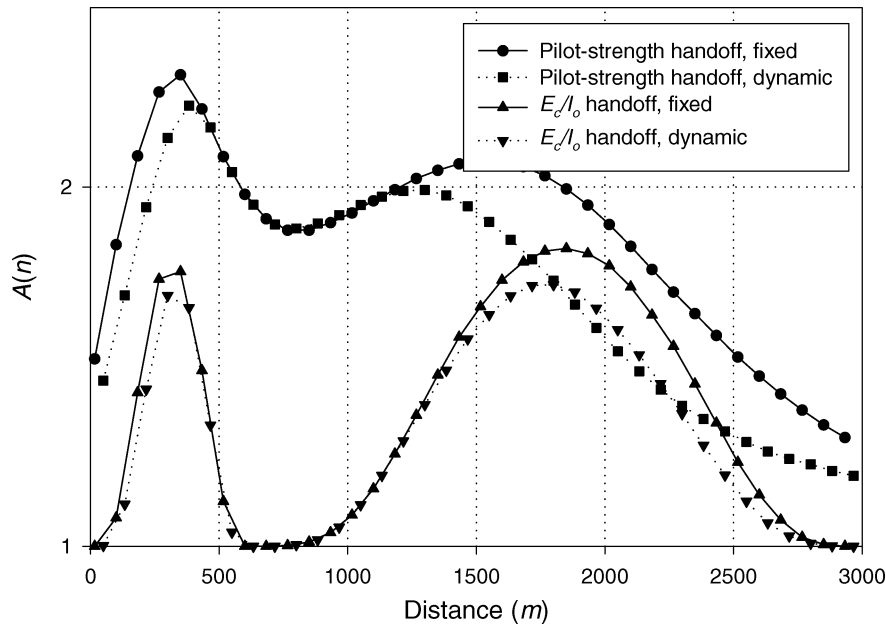

Fig. 13.   Handoff overhead comparison between pilot-strength and E_c/I_o based active set membership; $N = 13$ and $M = 12$.

forward link due to the presence of the microcell. This interference imbalance will impact the received E_c/I_o from each BS.

Figs. 12 and 13 compare the pilot signal power and E_c/I_o methods for determining active set membership, in terms of the handoff error probability and average number of BSs in active set. These E_c/I_o based results are obtained by assuming that $P_T(i)$ is the same for all BSs in the system (although this is an approximation). There are some significant differences in performance between received pilot power and E_c/I_o-based active set memberships. In particular, the E_c/I_o method requires much less overhead for a comparable handoff error performance. The observation may be attributed to the fact that E_c/I_o follows a slope up to $d^{-2\alpha}$ and has angular dependency. In either case, however, dynamic handoff parameter assignment yields a more efficient handoff mechanism than fixed handoff parameter assignment.

IV. CONCLUDING REMARKS

We have presented a new soft handoff analysis model for hierarchical CDMA systems. The model is constructed by first characterizing the interference imbalance in hierarchical CDMA deployments. The results are then applied to an MS tracking handoff model to obtain soft handoff performance measures such as handoff error probability and active set membership. It has been shown that our methodology (that considers reverse link interference imbalance) is superior to handoff analysis methods that rely on received pilot signal power only. We also showed that dynamic handoff parameter assignment, where handoff parameters are dynamically adjusted in response to the interference imbalance, yields a more efficient handoff mechanism than fixed handoff parameter assignment.

No handoff analysis method is perfect, including ours. In reality, soft handoff performance will depend on many factors,

including the particular set of time-variant channel impulse responses for every forward and reverse link in the entire system, the type of diversity that is employed (e.g., RAKE combining on the forward link and selection diversity on the reverse link), the spreading codes used, and synchronous versus asynchronous network operation. It will also depend on the particular algorithms used for receiver synchronization, channel and CIR estimation, power control algorithms, and many other factors. Nevertheless we have provided a reasonably simple soft handoff analysis for hierarchical CDMA systems where interference imbalance among cells can affect the system performance.

REFERENCES

[1] K. L. Yeung and S. Nanda, "Channel management in microcell/macrocell cellular radio systems," *IEEE Trans. Veh. Technol.*, vol. 45, pp. 601–612, Nov. 1996.

[2] B. Jabbari and W. F. Fuhrmann, "Teletraffic modeling and analysis of flexible hierarhcical cellular networks with speed-sentive handoff strategy," *IEEE J. Sel. Areas Commun.*, vol. 15, pp. 1539–1548, Oct. 1997.

[3] J. Shapira, "Microcell engineering in CDMA cellular networks," *IEEE Trans. Veh. Technol.*, vol. 43, pp. 817–825, Nov. 1994.

[4] J. S. Wu, J. K. Chung, and Y. C. Yang, "Performance improvement for a hotspot embedded in CDMA system," in *VTC'97*, May 1996, pp. 944–948.

[5] D. D. Lee, D. H. Kim, Y. J. Chung, H. G. Kim, and K. C. Whang, "Other-cell interference with power control in macro/microcell CDMA networks," in *VTC'96*, May 1996, pp. 1120–1124.

[6] J. Y. Kim, G. L. Stüber, and I. F. Akyildiz, "Macrodiversity power control in hierarchical CDMA cellular systems," in *IEEE Vehicular Technology Conf.*, Amsterdam, The Netherlands, Sep. 1999, pp. 2418–2422.

[7] D. H. Kim, D. D. Lee, H. J. Kim, and K. C. Whang, "Capacity analysis of macro/microcellular CDMA with power ratio control and tilted antenna," *IEEE Trans. Veh. Technol.*, vol. 49, pp. 34–42, Jan. 2000.

[8] W.-C. Chan, E. Geraniotis, and D. Gerakoulis, "Reverse link power control for overlaid CDMA ssystem," in *IEEE ISSSTA*, Parsippany, NJ, Sep. 2000, pp. 776–781.

[9] N. Zhang and J. M. Holtzman, "Analysis of a CDMA soft handoff algorithm," in *PIMRC'95*, Sep. 1995, pp. 819–823.

[10] S. Agarwal and J. M. Holtzman, "Modeling and analysis of handoff algorithms in multi-cellular systems," in *VTC'97*, May 1997, pp. 300–304.

[11] G. L. Stüber, *Principles of Mobile Communication*. Norwell, MA: Kluwer Academic, 1996.

[12] M. Zorzi, "On the analytical computation of the interference statistics with applications to the performance evaluation of mobile radio systems," *IEEE Trans. Commun.*, vol. 45, pp. 103–109, Jan. 1997.

[13] "Mobile station-base station compatability standard for dual-mode wideband spread spectrum cellular system," EIA/TIA, Tech. Rep. IS-95, 1992.

[14] A. J. Viterbi, A. M. Viterbi, K. S. Gilhousen, and E. Zehavi, "Soft handoff extends CDMA cell coverage and increases reverse link capacity," *IEEE J. Sel. Areas Commun.*, vol. 12, pp. 1281–1288, Oct. 1994.

[15] M. Gudmundson, "Correlation model for shadow fading in mobile radio systems," *Electron. Lett.*, pp. 2145–2146, Nov. 1991.

[16] N. D. Tripathi, J. H. Reed, and H. F. Vanlandingham, "Handoff in cellular systems," *IEEE Personal Commun. Mag.*, vol. 5, pp. 26–37, Dec. 1998.

[17] C. Chandra, T. Jeanes, and W. H. Leung, "Determination of optimal handover boundaries in a cellular netowrk based on traffic distribution analysis of mobile measurement reports," in *VTC'97*, May 1997, pp. 305–309.

John Y. Kim (S'97–M'02), photograph and biography not available at the time of publication.

Gordon L. Stüber (F'99) received the B.A.Sc. and Ph.D. degrees in electrical engineering from the University of Waterloo, ON, Canada, in 1982 and 1986, respectively.

Since 1986, he has been with the School of Electrical and Computer Engineering, Georgia Institute of Technology, Atlanta, where he is currently the Joseph M. Pettit Professor in Communications. His research interests are in wireless communications and communication signal processing. He is author of *Principles of Mobile Communication* (Norwell, MA: Kluwer Academic, 1996; 2001).

Dr. Stüber was a Corecipient of the Jack Neubauer Memorial Award in 1997 recognizing the best systems paper published in the IEEE TRANSACTIONS ON VEHICULAR TECHNOLOGY. He received the IEEE Vehicular Technology Society James R. Evans Avant Garde Award in 2003 recognizing his contributions to theoretical research in wireless communications. He was Technical Program Chair for the 1996 IEEE Vehicular Technology Conference (VTC'96), Technical Program Chair for the 1998 IEEE International Conference on Communications (ICC'98), General Chair of the Fifth IEEE Workshop on Multimedia, Multiaccess and Teletraffic for Wireless Communications (MMT'2000), General Chair of the 2002 IEEE Communication Theory Workshop, and General Chair of the Fifth International Symposium on Wireless Personal Multimedia Communications (WPMC'2002). He is a past Editor for Spread Spectrum with the IEEE TRANSACTIONS ON COMMUNICATIONS (1993–1998) and a past member of the IEEE Communications Society Awards Committee (1999–2002). He is currently an Elected Member of the IEEE Vehicular Technology Society Board of Governors (2001–2003, 2004–2006).

Ian F. Akylidiz (F'95) received the B.S., M.S., and Ph.D. degrees in computer engineering from the University of Erlangen-Nuernberg, Germany, in 1978, 1981, and 1984, respectively.

Currently, he is the Ken Byers Distinguished Chair Professor with the School of Electrical and Computer Engineering, Georgia Institute of Technology, Atlanta, and Director of the Broadband and Wireless Networking Laboratory. He is an Editor-in-Chief of *Computer Networks* and of *Ad Hoc Networks Journal*. He is a past Editor of *Journal of Cluster Computing* (1997–2001) and *Journal for Multimedia Systems* (1995–2001). His current research interests are in wireless networks, sensor networks, interplanetary Internet, and satellite networks.

Dr. Akyildiz is a Fellow of ACM. He is a past Editor for IEEE/ACM TRANSACTIONS ON NETWORKING (1996–2001) and IEEE RANSACTIONS ON COMPUTERS (1992–1996). He was Technical Program Chair of the 9th IEEE Computer Communications Workshop in 1994, for the ACM/IEEE Mobile Computing and Networking Conference (MOBICOM'96), IEEE Computer Networking Conference (INFOCOM'98), and IEEE International Conference on Communications (ICC'2003). He was General Chair for the premier conference in wireless networking, ACM/IEEE MOBICOM'2002, Atlanta, September 2002. He received the Don Federico Santa Maria Medal for his services to the Universidad of Federico Santa Maria in Chile in 1986. He was a National Lecturer for ACM from 1989 until 1998 and received the ACM Outstanding Distinguished Lecturer Award for 1994.

He received the 1997 IEEE Leonard G. Abraham Prize award (IEEE Communications Society) for his paper "Multimedia Group Synchronization Protocols for Integrated Services Architectures" in the IEEE JOURNAL OF SELECTED AREAS IN COMMUNICATIONS in January 1996. He received the 2002 IEEE Harry M. Goode Memorial award (IEEE Computer Society). He received the 2003 IEEE Best Tutorial Award (IEEE Communication Society) for his paper entitled "A Survey on Sensor Networks" in IEEE COMMUNICATION MAGAZINE in August 2002. He also received the 2003 ACM Sigmobile Outstanding Contribution Award and the 2004 Institute Outstanding Faculty Research Author Award from Georgia Institute of Technology in April 2004.

Boo-Young Chung, photograph and biography not available at the time of publication.